

Surface Modification of Laser Metal Deposited Ti-6Al-4V+10%Mo for Biomedical Applications

Arianna Ziemer
Department of Mechanical Engineering
Milwaukee School of Engineering
Milwaukee, WI 53202

Department of Mechanical Engineering
University of Johannesburg
Auckland Park, Johannesburg, South Africa 2006

Council for Scientific and Industrial Research – National Laser Center (CSIR-NLC)
Brummeria, Pretoria, South Africa

Advisors: Dr. Subha Kumpaty, Dr. Esther Akinlabi, Dr. Mutiu Erinosh, Dr. Sisa Pityana

Abstract

The main goal of the project was to observe characteristic changes in laser metal deposited Ti-6Al-4V + 10% Mo at varying scan speeds. Laser metal deposition is an additive manufacturing technique that begins with two hoppers that hold the powdered metals. The first hopper contained Ti-6Al-4V and the second hopper contained molybdenum. Ti-6Al-4V is a titanium alloy that consists of 6 wt% aluminum and 4 wt% vanadium. When the molybdenum was added to the Titanium alloy the hardness, biocompatibility, and corrosion resistance of the material were affected. The hoppers released the powder such that there was 90 wt% Ti-64 and 10 wt% Mo. The powders were deposited through a nozzle and a focused laser created a melt pool of the two metal powders onto a substrate. A three dimensional design program was used to create the path that the laser followed, depositing layers of the metal until the desired part was achieved. Five samples of the laser deposited Ti-6Al-4V + 10% Mo were completed at the CSIR National Laser Center in Pretoria, South Africa. The five samples consisted of scan speeds varying from 0.50 meters per minute up to 1.50 meters per minute, while the laser power remained at a constant 1700 Watts. The microstructure, micro hardness and corrosion resistance of the samples were the main focus in this project. Currently, Ti-64 is used in biomedical implants such as hip replacements. The results showed that the samples with the lower scan speeds had longer grain sizes, as the samples with the faster scan speeds had smaller grain sizes. The longer grain sizes created a stronger bond, so the slower scan speeds of 0.50 and 0.75 m/min are good for biomedical applications. Additionally, the scanning speeds of 0.50 and 1.50 m/min had low average Vickers Hardness values of 322 and 324, which is ideal because the soft material is less likely to cut into the bone surrounding the hip implant. The corrosion resistance test first revealed that the surface of the samples were rough. This roughness is important for osseointegration to be possible. When the samples were removed from the 7-day corrosion test, the grooves on the surface became deeper. All samples corroded to the same extent. Therefore, the scan speed of 0.50 m/min was considered overall to be ideal for biomedical applications. In the future, a higher laser power should be used in order to successfully integrate the powdered metals by fully melting the molybdenum particles. Additionally, scanning speeds lower than 0.50 m/min should be further researched.

Keywords: Laser, Metal, Biomedical

1. Introduction

The purpose of this project was to research Ti-6Al-4V +10% Mo alloy when it is laser metal deposited onto a Ti-64 substrate at increasing scan speeds for application in biomedical implants. The Ti-64 +10% Mo alloy contains 80 wt% titanium, 6 wt% aluminum, 4 wt% vanadium and 10 wt% molybdenum. Three main studies were done in order to determine which scan speed is optimal for biomedical applications. First, the microstructure of the samples were observed and compared, then the Vickers hardness at each scan speed was determined and finally the corrosion resistance of each sample was considered as if it were implanted into the human body.

2. Background

2.1 Laser Metal Deposition

Laser Metal Deposition is an additive manufacturing technique that begins with a 3-dimensional model for a desired part. The model for this part is split up into thin horizontal layers. These layers are used to create a path for the laser to follow. Along that path, a focused laser creates a melt pool on a substrate. Powdered metals are fed through two hoppers and then deposited onto the melt pool. As the deposit cools it becomes fusion bonded to the metallic substrate¹. Simultaneously, Argon gas is used to shield the entire process from oxidation. The laser beam continues this process as it follows the path created. The paths are continued atop each other layer by layer, until the desired part is completed. A representation of this process is shown in figure 1.

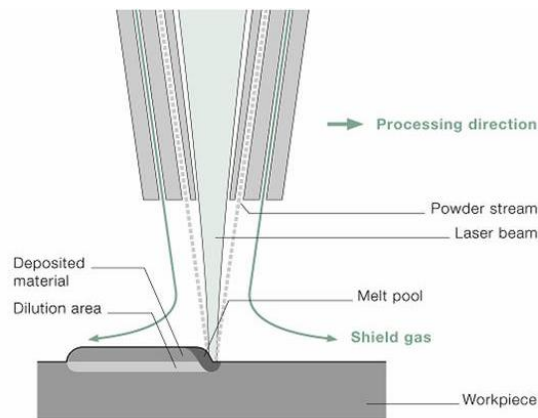


Figure 1: Representation of the LMD Process¹

2.2 Biomedical Applications

The Ti-6Al-4V alloy is commonly used to create biomedical implants such as total hip replacements. This is where the ball of the femur is removed and replaced with an artificial ball, known as a biomedical hip replacement². Hip replacements must have a good balance between ductility and strength in order to withstand daily stresses of the human body movement. A lower Vickers hardness value is ideal because the material will be ductile and able to resist stress yielding, similar to the surrounding femur bone.

Currently, hip replacements are being produced from various powder metallurgy forming techniques such as wrought bar stock of Ti-6Al-4V being CNC machined³. Additionally, each hip replacement lasts for approximately 20 years. After the 20 year time period a repeat hip replacement is necessary. Due to the increase in age of the patient and the complexity of the surgery, this repeat hip replacement often results in a higher risk procedure and longer hospitalization⁴. If the corrosion resistance of the material could be improved upon, the need for repeat hip replacements could be eliminated.

2.3 Material Properties

Ti-6Al-4V has a low electrical conductivity which leads to a high corrosion resistance. Due to this high resistance to corrosion within the human body, titanium alloys have been used for biomedical applications since the early 1970's⁵. The addition of molybdenum creates changes in the characterization of the alloy. Ti-64 has a melting point of 1604-1660 °C⁷, which is much lower than molybdenum at 2623 °C⁸. This results in unmelted molybdenum particles when integrating the two powdered metals together. Ti-64 has an average Vickers hardness value of 349⁷, while molybdenum has a lower Vickers hardness of 230⁸. It is expected that the addition of molybdenum will lower the Vickers hardness of the deposit and bring it slightly closer to the 45-50 Vickers hardness of the surrounding Femur bone for biomedical hip replacements⁶. Additionally, Ti-64 has an average modulus of elasticity of 113.8 GPa⁷, while molybdenum has an average modulus of elasticity of 330 GPa⁸, therefore it is expected that the addition of molybdenum will create a more ductile material. On the other hand, the density of Ti-64 is 4.42 g/cm³ and the density of molybdenum is 10.2 g/cm³. This higher density leads to the prediction that the addition of molybdenum may unfortunately create a heavier implant^{7,8}.

3. Methodology

3.1 Sample Preparation

First, two hoppers were filled with two separate powdered metals. One was filled with Ti-6Al-4V, while the other was filled with molybdenum. The control panel was adjusted such that the Ti-64 has a 3.6 rpm flow rate, while the molybdenum had a 0.4 rpm flow rate. This ensured that the alloy would be 90% Ti-64 and 10% molybdenum. Additionally, the laser was set to a power of 1700 Watts with 6 tracks overlapping each other by 50%. The laser utilized five different laser scanning speeds, starting at 0.50 m/min and increased by 0.25 m/min increments, until it reached 1.50 m/min, as displayed in table 1. Figure 2 is an image of the five samples created. Visually, it can be observed that the slower scanning speeds produced a thick deposit, which gradually became thinner as the scan speeds increased.

Table 1: Laser Specifications Matrix

Sample Number	Laser Power (W)	Scanning Speed (m/min)	Powder Flow Rate (rpm)	
			Ti-64	Mo
1	1700	0.50	3.6	0.4
2		0.75		
3		1.00		
4		1.25		
5		1.50		

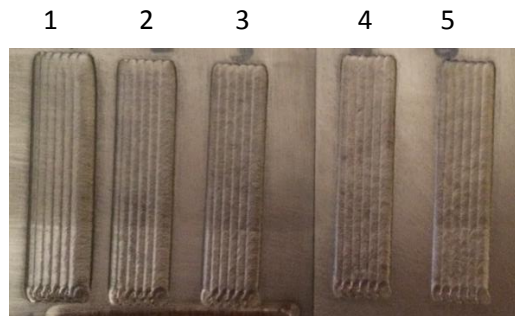


Figure 2: Laser Metal Deposited Samples (Samples 1-5 Left to Right)

3.2 Cutting

A total of ten samples were cut, two from each scanning speed. The cutting was done using a Mecatome T300 cutting apparatus equipped with a Struers 20S25 cutting wheel, with all settings based on the Struers 2016 cutting handbook⁹. Each sample was cut based on the red lines in figure 3, resulting in each sample measuring approximately 10mm x 10mm x 7mm.

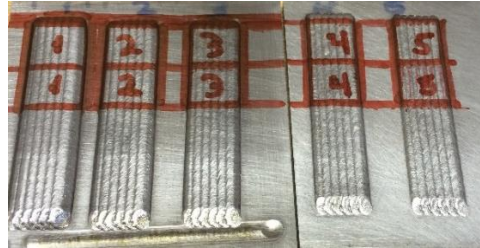


Figure 3: Cutting Outline of (Samples 1-5 Left to Right)

3.3 Mounting

Cross-sections from each scan speed and the substrate were mounted in a PolyFast hot mounting resin with a carbon filler. Using a Struers CitoPress-1 Pneumatic Hot Mounting Press, each sample was lowered into the apparatus with the cross-section facing down. The 20 mL of the PolyFast powder was added and the ram was tightened. First the mounting press heats the powder to 180°C while applying 250 bars of pressure for 3.5 minutes. Next, water cooled the melted powder into a solid cylindrical shape with the cross-section exposed. This can be seen for each sample in figure 4. This type of resin is designed for excellent edge retention in the samples after mounting. The mounting is necessary to increase ease of handling, both by hand and for use in grinding machines.



Figure 4: Five Mounted Cross-sections (Samples 1-5 Left to Right)

3.4 Grinding and Polishing

After mounting, each sample went through a three-step grinding and polishing process on a Struers Polishing Machine. First, each sample was rough grinded for ten minutes using a disk of Silicon Carbide Paper #320 at 250 rpm while under a pressure of 10 N force and lubricated by water to allow the grinding disk to spin smoothly under the samples. This rough grinding allowed for excess Polyfast and uneven surfaces to be removed from the mounted samples. The second step was a fine grinding process in order to remove large imperfections on the sample. Each sample was grinded for 8 minutes with a MD Large Plate at 150 rpm while under a force of 10 N. The samples were lubricated with a Diapro suspension, which consists of diamond particles to achieve precise grinding. Finally, the third step was to polish the sample in order to remove all small scratches and imperfections. Each sample was polished with a MD Chem polishing disk at 150 rpm, under a force of 10 N while being lubricated with an OP-S silica suspension. The polishing step was repeated in 5 minute intervals until a mirror like finish was visible to the naked eye.

3.5 Microstructural Evaluation

According to the Struers Application Notes handbook, titanium can exist in two different forms. First, a closed packed hexagonal structure that is created at low temperatures is considered to be the α phase⁹. The material can then undergo

a change in structure when heated to 882°C. The rise in temperature creates the β phase, a body centered cubic structure. Thus, this change in titanium allows for the allotropic material to consist of both α and β phases⁹.

3.5.1 Etching

According to the Struers Application Notes handbook on metallographic preparation of titanium, the most common chemical etchant for titanium alloys is Kroll's reagent⁹. The Kroll's reagent was prepared by mixing 100mL of water, 1mL of Hydrofluoric Acid and 2mL of Nitric Acid. This reagent is used to color the β phase dark within the grains of the alloy, allowing the distinction between the α and β phases to be visible when under a microscope⁹. The surface of each sample was submerged into Kroll's reagent for 5 second intervals until the β phase in the grains was visible under a light optic microscope.

3.5.2 Light Optic Microscope

In order to view the microstructures of each sample, the Olympus OM was used. The Olympus OM is a light refracting microscope that holds a mirror which reflects adjustable light rays onto the sample and then through the objective lenses. The objective lenses then magnify the image so it appears enlarged when viewed from the eyepiece. Images of each sample were observed at 50x, 100x, 200x and 500x magnifications. As the magnifications increased, the details in the microstructures became better defined.

3.5.3 Scanning Electron Microscopy

The scanning electron microscope (SEM) was also used to view the microstructure of each sample. First, the samples were placed in the apparatus. Rather than using light rays, the SEM makes use of a focused electron beam. The beam interacts with the atoms on the surface of the sample, this interaction produces signals that visually displays the surface of the sample.

3.5.4 Energy Dispersive Spectroscopy

Energy Dispersive Spectroscopy (EDS) is part of the Scanning Electron Microscopy. The difference is that EDS takes the signals from the focused electron beam and gathers information on the surface composition. Thus, EDS can be used to determine exact percentages of different elements at the surface of the sample.

3.6 Vickers Hardness Testing

Hardness is a measurement of a material's ability to resist deformation when a load is applied. The Vickers hardness test uses a diamond indenter in the shape of square based pyramid with an angle of 136° between opposite faces¹⁰. The diamond indenter is used to penetrate the sample at a force of 500kg_f, or 4.9 N for 15 seconds. The first indent was made on the top of the deposition of the sample, from there the following indents were made 200 micrometers apart until there where a total of 20 indents. The diameter of each diagonal across the base of the pyramidal indentation are measured in millimeters and labeled as d_1 and d_2 . The Vickers hardness is calculated by using equations 1 and 2, where "F" is the force in kg, "D" is the average diameter in millimeters and "VH" is the Vickers hardness measurement¹⁰.

$$VH = \frac{1.8544 F}{D} \quad (1)$$

$$D = \frac{d_1 + d_2}{2} \quad (2)$$

3.7 Corrosion Resistance Testing

In order to observe the corrosiveness of the samples, the remaining five unmounted samples were placed into a jar and submerged into a Hanks Balanced Salt Solution, which imitates natural body fluid. The jar was then sealed with a rubber cork to protect the Hank’s Solution from condensation. The jar was then placed into a Memmert water bath system. The water bath was held at 37.0°C, the temperature of the human body, for seven consecutive days. The samples were then reviewed using the Scanning Electron Microscope to identify any corrosion that had occurred on the surface.

4. Results and Discussion

4.1. Light Optic Microscope (LOM) Observations

At a magnification of 50x, sample 3 was observed to reveal a clear image where the deposited Ti-6Al-4V + 10% Mo is visible atop of the Ti-64 substrate. Figure 5 shows that the deposit is homogenous throughout the sample, including visible black spots which are viewed at closer magnification in section 4.2. The interface is a clear line that shows where the deposit comes into contact with the substrate and creates a bond. Additionally, the area where the heat produced by the laser alters the substrate is labeled as the “heat affected zone” in figure 5. When sample 4 was observed under the LOM, long columnar grains became apparent. There is a clear distinction between the α and β grains. The β grains were colored dark from the etching, allowing for the lighter α grains to also become visible in figure 6. Figure 6 also emphasizes the 50% overlap between the tracks, with one deposited track laying atop the previous track, separated by the deposition line that is shown as a white dotted line.

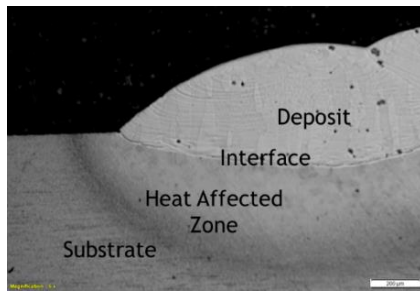


Figure 5: Sample 3 at 50x Magnification

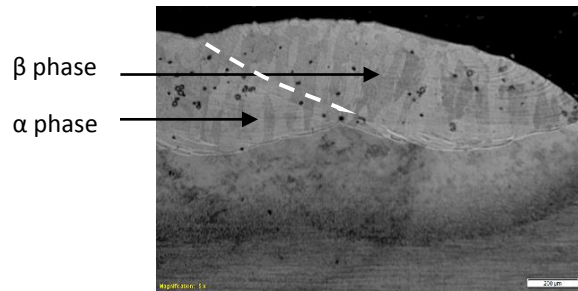


Figure 6: Sample 4 at 50x Magnification

As the magnification was increased, the grains became detailed enough to allow for measurement. The columnar grains from sample 1 with the slowest scan speed and sample 5 with the fastest scan speed were measured in micrometers, as shown in figures 7 and 8 respectively.

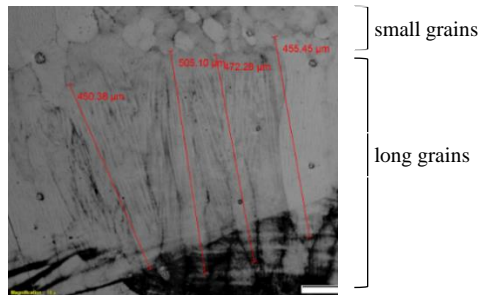


Figure 7: Sample 1 at 100x Magnification

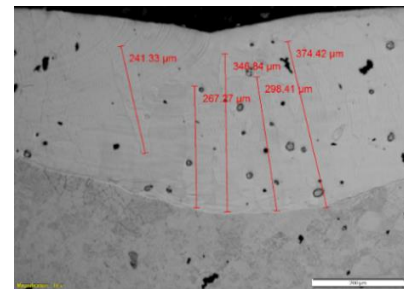


Figure 8: Sample 5 at 100x Magnification

First, figure 7 shows smaller grains near the top of the image. The small grain size is due to the rapid cooling at the top of the sample, while the middle of the deposit cools slowly. It is clear to see that the grains in sample 1 are longer than the grains in sample 5 of figure 8. In order to compare the grain sizes, the average grain size of each sample are represented in figure 9.

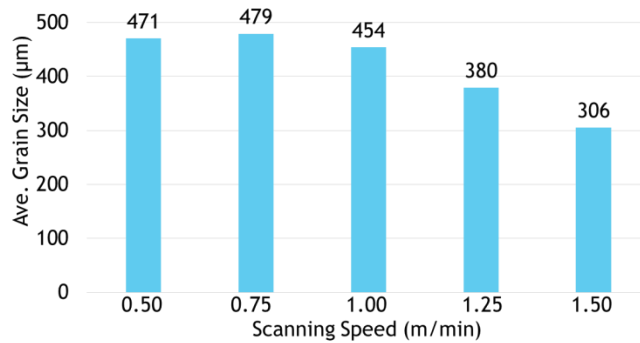


Figure 9: Grain Size Comparison Chart (Samples 1-5 Left to Right)

Samples 1 and 2 have similar grain sizes at 471 and 479 micrometers long at scan speeds of 0.50 m/min and 0.75 m/min respectively. The grain sizes decreased while the scan speeds increased, reaching a grain size of about 306 micrometers at a scan speed of 1.50 m/min. Thus, the grain sizes have an inverse relationship with the scanning speeds. This inverse relationship can be linked to the fact that the slower scanning speeds produced a thick deposit, allowing for longer columnar grains to form. Since the longer grains have more contact with each other, a stronger bond is created¹¹. Therefore, samples 1 and 2 with lower scan speeds are ideal for biomedical applications.

4.2 Scanning Electron Microscopy Observations

One of the many dark spots, mentioned in section 4.1, was viewed under the scanning electron microscope at a magnification of 1000x in figure 10. Towards the top of the image there are white thin lines visible; these are the grain boundaries in the microstructure. In the center of the image, the dark spot is revealed to actually be a large white circular spot. It was hypothesized that this spot is an unmelted molybdenum particle; this was looked into further by the energy dispersive spectroscopy. Below the white particle is a thick white interface where the deposit makes contact with the substrate. Finally, the bottom of the image shows part of the heat affected zone (HAZ) in the substrate.

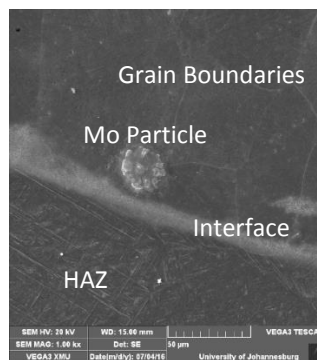


Figure 10: Sample 3 Under SEM at 1000x Magnification

4.3 Energy Dispersive Spectroscopy Observations

In order to verify the white spots as molybdenum particles, a grouping of the particles in Sample 4 were observed. The energy dispersive spectroscopy was set to determine the elements in the surrounding area displayed as spectrum 2 in figure 11. Table 2 shows the percentage of each element found in the surrounding area. The weight percentage match the expectation of Ti-6Al-4V +10% Mo fairly well.

Table 2: EDS Dark Area Weight Matrix

Element	Weight %
Ti	81.30
Mo	9.64
Al	5.70
V	3.36
Total	100.00

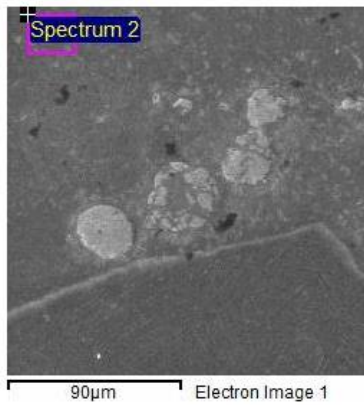


Figure 11: Sample 4 EDS Dark Area

The EDS was then shifted to the white particles displayed as spectrum 3 in figure 12, in order to verify the predication. Based on table 3, the light area consists of 99.72 wt% molybdenum and only 0.28 wt% titanium. This confirmed the hypothesis that the white areas are unmelted molybdenum particles.

Table 3: EDS Light Area Matrix

Element	Weight %
Ti	0.28
Mo	99.72
Total	100.00

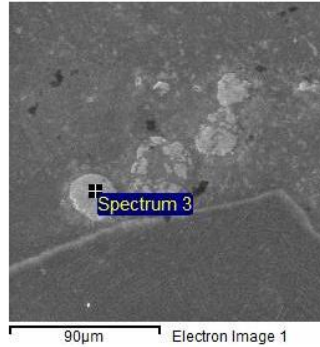


Figure 12: Sample 4 EDS Light Area

These unmelted molybdenum particles are likely to produce imperfections in a hip replacement. In order to fully melt these particles, the laser power could be increased, producing more heat, melting the particles and successfully integrating the two powdered metals together.

4.4 Vickers Hardness

Generally, a balance must be achieved between materials being too hard, in which they would become brittle and break, and being too ductile, in which they would not maintain the original shape over time. The average Vickers hardness of the deposit from each sample is shown in figure 13. Samples 2-4 show similar high values ranging from 353 to 357 for Vickers hardness. Sample 1 with the slowest scan speed of 0.50 m/min and sample 5 with the highest scan speed of 1.50 m/min both have the lowest hardness values of 322 and 324 respectively. The difference between the averaged values is approximately 32. While this difference is large enough to recognize, it would take a difference of at least 40 to see a significant impact when implementing the hip replacement. On the other hand, the lower hardness values are ideal because they are slightly closer to that of natural bone. The higher hardness values indicate that the implant is more likely to cut into the surrounding bone.

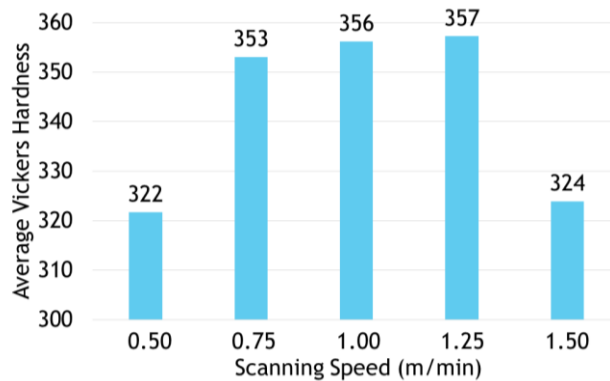


Figure 13: Average Vickers Hardness (Samples 1-5 Left to Right)

4.5 Corrosion Resistance

An image of sample 1 with a scan speed of 0.50m/min before it was placed in the Hank's solution is shown in figure 14. The surface appears to be rough and spongy; this roughness is essential for osseointegration, which allows the body's cells to attach and grow onto the implant. Figure 15 shows sample 1 after the 7-day corrosion resistance test was completed. It can be observed that the grooves had grown deeper and some of the material has been pulled out. This proves that some corrosion has occurred, however, the change in weight was unmeasurable. Since the change in weight was insignificant, a predication cannot be made but, it can be said that there was not extreme corrosion after seven days. Each of the 5 samples appeared to have corroded to the same extent. In order to predict the corrosion

resistance further, the test would have to be continued for a longer period of time with measurements of the change in weight recorded.

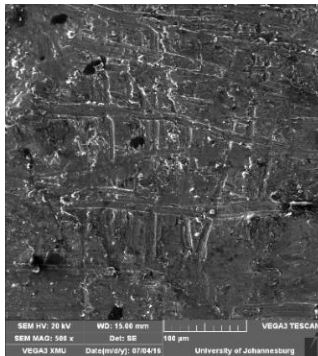


Figure 14: Sample 1 Before Corrosion Resistance

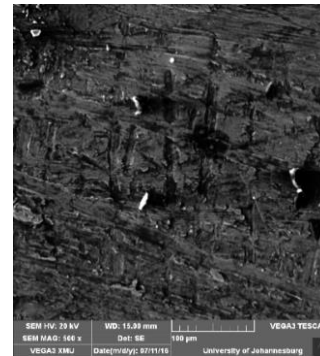


Figure 15: Sample 1 After Corrosion Resistance

5. Conclusion

Characteristics of laser metal deposited Ti-6Al-4V +10% Mo at varying scan speeds were considered. In conclusion, scanning speeds of laser metal deposited Ti-6Al-4V + 10% Mo have an inverse relationship with grain size. The longer grain sizes created a stronger bond, determining that samples 1 and 2 with a scan speeds of 0.50 m/min and 0.75 m/min have the ideal grain structure for biomedical applications. Furthermore, samples 1 and 5 with scan speeds of 0.50 m/min and 1.50 m/min respectively, had low Vickers hardness values of 322 and 324. The lower hardness values are ideal for biomedical applications because the material is less likely to cut into the surrounding bone. Each sample revealed a similar amount of corrosion after being immersed in the Hank's solution for seven days. Unfortunately, the difference in weight loss was unmeasurable. In the future, the corrosion resistance test should continue over a longer period of time so that the weight loss can be measured. Additionally, a higher laser power should be used in order to create the heat needed to fully melt the molybdenum particles. Finally, since the slow scan speeds demonstrated the desired characteristics, lower scan speeds should be considered.

6. Acknowledgments

The author is grateful to the National Science Foundation (NSF) for funding the project, Milwaukee School of Engineering (MSOE) for hosting the program, the Council for Scientific and Industrial Research (CSIR) for creating the LMD samples and the University of Johannesburg (UJ) for use of laboratory equipment. Special thanks are given to Dr. Subha Kumpaty, Dr. Esther Akinlabi, Dr. Sisa Pityana, Betty Albrecht, Opeluwa Dada, Dr. Mutiu Erinsho, UJ students and staff and all of the REU Participants.

This material is based upon work supported by the National Science Foundation under Grant No. EEC-0540834. Any opinions, findings, and conclusions or recommendations expressed in this material are those of the author(s) and do not necessarily reflect the views of the National Science Foundation.

7. References

1. LPW Technology. "Laser Metal Deposition." LPW. LPW Technology, 2016. Web. 09 Aug. 2016.
2. Arthritis Research UK. "Total Hip Replacement." Arthritis Information. N.p., 2016. Web. 09 Aug. 2016.
3. L. E. Murr, S. A. Quinones, S. M. Gaytan, M. I. Lopez, A. Rodela, E. Y. Martinez, D. H. Hernandez, F. Medina and R. B. Wicker, "Microstructure and Mechanical Behavior of Ti-6Al-4V Produced by Rapid-Layer Manufacturing, for Biomedical Applications," *The Mechanical Behavior of Biomedical Materials*, pp. 20-32, 2006.

4. Arthritis Research UK. "Revision Surgery." Arthritis Information. N.p., 2016. Web. 09 Aug. 2016.
5. Sidambe, Alfred T. "Biocompatibility of Advanced Manufactured Titanium Implants—A Review." *Materials* 7.12 (2014): 8168-188. Open Access. Web. 9 Aug. 2016.
6. Cerbio Tech. Ceramic Material and Process for Manufacturing. Patent Services. IFI CLAIMS Patent Services, 10 July 2003. Web. 9 Aug. 2016.
7. MatWeb LLC. "Titanium Ti-6Al-4V Annealed." ASM Material Data Sheet. ASM Aerospace Specifications Metals Inc., n.d. Web. 09 Aug. 2016.
8. IMOA. "Molybdenum Properties." IMOA. International Molybdenum Association, n.d. Web. 09 Aug. 2016.
9. Taylor. Bill, Weidmann. Elisabeth. *Metallographic Preparation of Titanium*. Denmark: Taylor. Bill, Weidmann. Elisabeth, n.d. Print.
10. England, Gordon. "Hardness Test." *Thermal Spray Coatings* (2013): 1-13. Gordon England. Surface Engineering Forum, 2013. Web. 9 Aug. 2016.
11. Wu, Xinhua, Jing Liang, Junfa Mei, C. Mitchell, P.S. Goodwin, and W. Voice. "Microstructures of Laser-Deposited Ti-6Al-4V." *Materials and Design* 25.2 (2004): 137-44. Science Direct. Web. 9 Aug. 2016.